Contents lists available at ScienceDirect

Food and Bioproducts Processing

journal homepage: www.elsevier.com/locate/fbp

Biosynthesis of silver nanoparticles as catalyst by spent coffee ground/recycled poly(ethylene terephthalate) composites

Dave Mangindaan[a], *Guan-You Lin*[b], *Chia-Jung Kuo*[c], *Hsiu-Wen Chien*[b,c,*]

[a] *Professional Engineering Program Department, Faculty of Engineering, Bina Nusantara University, Jakarta, 11480, Indonesia*

[b] *Department of Chemical and Materials Engineering, National Kaohsiung University of Science and Technology, Kaohsiung, Taiwan*

[c] *Photo-Sensitive Material Advanced Research and Technology Center (Photo-SMART Center), National Kaohsiung University of Science and Technology, Kaohsiung, Taiwan*

ARTICLE INFO

Article history:
Received 7 November 2019
Received in revised form 30 January 2020
Accepted 26 February 2020
Available online 3 March 2020

Keywords:
Spent coffee grounds
Plastic bottles
Silver nanoparticles
Catalysts
4-Nitrophenol
Green chemistry

ABSTRACT

Spent coffee ground (SCG) and poly(ethylene terephthalate) (PET) bottles are common wastes in the beverage industries. In this study, SCG and PET sheets from waste PET bottles were utilized to prepare PET/SCG composites. Those composites were embedded with silver nanoparticles (AgNPs) prepared from $AgNO_3$ solutions (0–100 mM) without addition of catalyst or reducing agent, to be AgNPs@PET/SCG sheets. The generation of AgNPs was confirmed by field emission scanning electron microscopy (FESEM) and X-ray diffraction (XRD). According to inductively coupled plasma (ICP) analysis, the loaded amount of AgNPs on PET/SCGs was in the range of 0.9–7.3 $\mu g/cm^2$. The catalytic performance and kinetics of AgNPs@PET/SCGs for the reduction of 4-nitrophenol with $NaBH_4$ was studied, where 100% conversion can be reached in 20 min. The prepared AgNPs@PET/SCGs sheets allow easy separation from the reaction media, and can be reused for at least seven cycles while maintaining >90% conversion rate. The durable and reusable AgNPs@PET/SCGs made from waste materials may provide a promising alternative for further industrial applications.

1. Introduction

Spent coffee grounds (SCGs) are the main by-products resulted from coffee brewing process, and generated million tons annually. Although SCGs are considered as waste, but actually there are a lot of biofunctional components in SCGs, e.g. fatty acids, lignin, cellulose, hemicellulose, and polyphenols (Campos-Vega et al., 2015; Kovalcik et al., 2018), which are very potential to be valorized. The value-adding processing of SCGs (as well as of food wastes, in general (Xiong et al., 2019)) is projected to drive the reduction of the volume of organic waste dumping, thus alleviation in greenhouse gas production in landfills, then potentially opens new economic opportunity of SCGs-based chemicals or commodities, and therefore resulting in sustainable development.

In order to support the aforementioned sustainable development based on SCGs, there are several existing methods for the utilization of SCGs. The simplest method is the use of pristine SCGs without additional processing for application in wastewater treatment (i.e. as adsorbents for removal of heavy metal ions (e.g. Cu(II), Cr(IV) (Kyzas, 2012), Pb(II) and Hg(II) (Chavan et al., 2016) and pharmaceutical contam-

* *Corresponding author at*: Department of Chemical and Material Engineering, National Kaohsiung University of Science and Technology, Kaohsiung, 80778, Taiwan.
E-mail address: hsiu-wen.chien@nkust.edu.tw (H.-W. Chien).

https://doi.org/10.1016/j.fbp.2020.02.008

inants (e.g. metamizol, acetylsalicylic acid, acetaminophen, and caffeine) (Lessa et al., 2018)). Besides the application of the untreated SCGs, there is also the bulk physical transformation of SCGs. They might be converted to be charcoal for adsorbent of aqueous heavy metal ions (Yeung et al., 2014) or to be activated carbon for methane storage (Kemp et al., 2015). Finally SCGs can be functionalized by coating using polyethyleneimine for successive extraction of As(V), Cu(II) and P(V) (Hao et al., 2017), or by the newly developed bio-based decoration of silver nanoparticles for highly efficient antibacterial materials (Chien et al., 2019). Environmentally-benign methods for synthesis of nanoparticles have been extensively reviewed elsewhere (Sharma et al., 2009; Iravani, 2011; Mittal et al., 2013; Duan et al., 2015).

One of the bio-based approaches for the synthesis of metal nanoparticles is the use of plant extracts as biological systems that perform as the reducing and capping agent (Iravani, 2011; Mittal et al., 2013; Saratale et al., 2019). Several previous studies employed coffee extract to synthesize nanoparticles, specifically silver nanoparticles (Nadagouda and Varma, 2008; Metz et al., 2015; Dhand et al., 2016), and additionally Pd nanoparticles (Nadagouda and Varma, 2008). It is proposed that the hydroxyl and carboxyl groups of the polyphenolic compounds of the plant extracts will form a complex with the metal salt solution, and perform the reduction mechanism of the complex to be metal atoms. Furthermore, the metal nuclei will further grow resulting in the production of metal nanoparticles (Iravani, 2011; Mittal et al., 2013; Thanh et al., 2014; Veisi et al., 2018). For the case of SCGs, the identified polyphenolic compounds in SCGs that might be responsible for the aforementioned mechanism are chlorogenic acid and its derivatives, caffeoylquinic acids, feruloylquinic acids, and *p*-coumaroylquinic acids (Mussatto et al., 2011; Zuorro and Lavecchia, 2012).

Recently, there is an increasing number of reports of the preparation of catalysts from waste materials (Klose et al., 2000; Balakrishnan et al., 2011; Bennett et al., 2016). Valorizing waste materials to fabricate the value-added catalysts not only reduces waste materials in landfills, but also serves as cost effective raw material. The manufactured catalysts from waste materials must be carefully designed and prepared in order to generate not only highly active and stable catalysts, but also simple and safe to collect. It would be greatly appreciated if the production processes of catalyst from waste materials is as environmentally-benign as possible and do not burden any additional environmental issues. Beverage industries produce not only SCGs, but also waste PET bottles. It would be a good alternative to synergistically use these wastes (SCGs and PET bottles) for producing catalyst.

To the best of our knowledge, our recent report is the only study (Chien et al., 2019) on the utilization of SCGs as bio-based system for direct synthesis of metal nanoparticles without additional dispersing, capping or reducing agent, at room temperature. Therefore, it would be exciting to discover the potentials of the newly established class of biosynthesized metal nanoparticles for sustainable development applications. In this study, we developed SCGs-derived AgNPs attached on the surface of SCG powders immobilized in waste PET sheets for easier collection and better protection, stated as AgNPs@PET/SCGs. They were created without additional reducing or capping agent, and were implemented for the catalytic reduction of a model organic pollutant (4-nitrophenol (4-NP)). In addition to the proof of concept, this study is important to promote the reduction of SCGs waste, reusing PET bottles, and valorize them as value-added catalysts for sustainable environmental applications. This study is illustrated in Fig. 1.

2. Experimental methods

2.1. Materials

Trifluoroacetic acid (TFA, 99%) and silver nitrate ($AgNO_3$, >99.9%) were purchased from Alfa Aesar. *N*-Pentane (≥99%) was bought from Sigma-Aldrich. 4-Nitrophenol (99%) and sodium borohydride ($NaBH_4$, >98%) were received from Acros Organics. Nitric acid (HNO_3) was received from Fluka, while sodium chloride (NaCl) was purchased from Shimakyu's Pure Chemicals Co., Ltd.

2.2. Preparation of SCGs and PET bottles

The SCGs were collected and washed three times with DI water to remove the impurity or residue, which was further defatted via a solvent extraction process with n-pentane according to the previous procedure (Chien et al., 2019). The defatted SCGs were further ground by using an electric grain mill, and sieved through a 30 mesh sieve. The waste PET bottles were employed as a material for polymeric matrix, where those bottles were first cleaned up, dried and cut by 0.5 × 0.5 cm^2.

2.3. Fabrication of the PET/SCGs composites

The PET/SCGs composites were fabricated by using a film casting process. The casting solutions were prepared by dissolving a 15 (w%) of PET in TFA, and the mixtures were stirred for 6 h at room temperature. Subsequently, 15 (w%) of SCGs and 22.5 (w%) of NaCl salt sieved through a 30 mesh sieve were added with continuous stirring until the solution was completely clear and homogeneous. The NaCl powders were added into the solution in order to make the porous composites. The casting solution was then poured onto a clean glass plate at room temperature. The solution was cast on a glass plate using a casting knife with a thickness gap set at 350 μm. Immediately after casting, the glass plate with the cast film was dipped into distilled water at room temperature. After a few minutes, a thin composite film separated itself from the glass. The fabricated PET/SCGs composites were washed with distilled water and kept in a water bath before evaluation. The average thickness of the PET/SCGs composites was measured to 396 μm ± 33 μm.

2.4. Silver loaded PET/SCGs composites

AgNPs were loaded on the surface of the PET/SCGs composites by directly exposing 5 × 5 cm^2 of PET/SCGs composites into 10 mL aqueous $AgNO_3$ solution with concentration of 1, 10, 50, or 100 mM with continuous stirring at room temperature for 6 h, and were washed with DI water to remove the residues or excess reagents, and then dried in an oven at 50 °C overnight. The PET/SCGs into 1 mM, 10 mM, 50 mM, and 100 mM of HNO_3 aqueous solution to load AgNPs were named as 1_AgNPs@PET/SCGs, 10_AgNPs@PET/SCGs, 50_AgNPs@PET/SCGs, and 100_AgNPs@PET/SCGs composites, respectively.

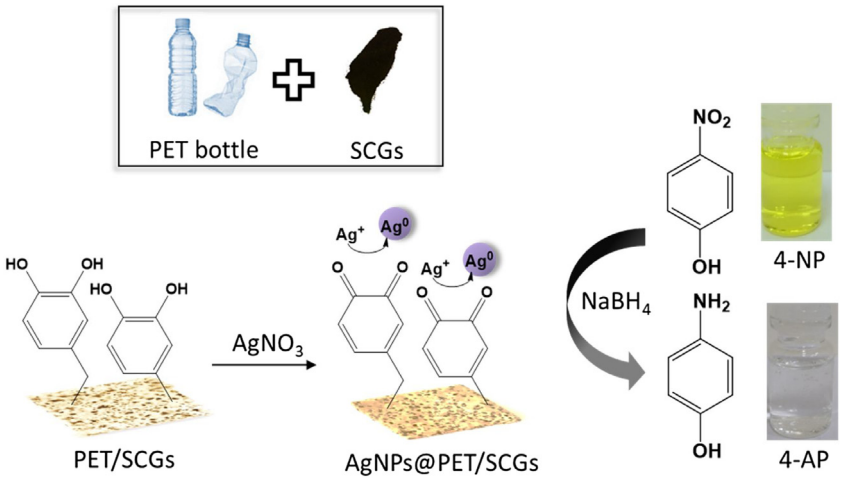

Fig. 1 – Schematic diagram illustrating the production of AgNPs@PET/SCGs catalysts. The phenolic compounds in SCGs play a role in reducing agents to reduce Ag^+ ions to Ag^0. The generated silver nanoparticles (Ag^0) has a catalytic activity towards 4-nitrophenol reduction.

2.5. *Characterizations*

Morphology of AgNPs@PET/SCGs composite was examined by field emission scanning electron microscopy (FESEM), JEOL JSM-6701F, Japan. All samples were platinum-coated by a sputter coater before the observation. X-ray diffraction (XRD) analysis for studying the crystalline nature and the diffraction patterns were recorded in the scanning mode on a high resolution X-ray diffractometer (Bede D1). The process was operated at 40 kV and with a current of 40 mA with Cu/Kα radiation (λ = 1.5405 Å) in the range of 10°–80° in 2θ angles with a scanning speed of 0.05° s^{-1}.

2.6. *Quantification of silver loading*

The silver content was detected by using inductively coupled plasma optical emission spectrometer (ICP-OES, Thermo Scientific iCAP 700). The AgNPs on the PET/SCGs were digested in nitric acid and then diluted by using DI water. After passing through a 0.22 μm polyethersulfone (PES) filter, the samples were analyzed for silver content. Three replicates were used to analyze the silver concentration.

2.7. *Catalytic activity assays of AgNPs@PET/SCGs composites*

The catalytic activity of was evaluated by reducing 4-nitrophenol (4-NP) to 4-aminophenol (4-AP) in a quartz cell at room temperature. Specifically, 15 mL of 4-NP (0.08 mM) was mixed with 3.3 mL $NaBH_4$ solution (0.64 M). After adding 1 × 1 cm^2 of AgNPs@PET/SCGs composites, the reactions were monitored through the absorbance at 400 nm by using UV–vis spectrophotometer (ChromTech CT-2800). The PET/SCGs composites without AgNPs-loading were employed as control group.

2.8. *Reuse test of AgNPs@PET/SCGs composites*

The recyclability of the 100_AgNPs@PET/SCGs composites on consecutive 4-NP reduction reactions was evaluated. The 1 × 1 cm^2 of composites was immersed into 15 mL of 4-NP (0.08 mM) was mixed with 3.3 mL $NaBH_4$ solution (0.64 M). The reactions within 20 min were then monitored through the absorbance at 400 nm by using UV–vis spectrophotometer. Upon completion of each reduction reaction, the composites were recovered by washing DI water three times and dried for the next runs. Three replicates were used to test the reuse experiments.

Table 1 – Particle size and content of AgNPs in AgNPs@PET/SCGs samples.

Samples	$AgNO_3$ (mM)	Particle size (nm)	AgNPs content (μg/cm^2)
PET/SCGs	0	–	–
1_AgNPs@PET/SCGs	1	34.61 ± 5.37	0.938 ± 0.255
10_AgNPs@PET/SCGs	10	38.84 ± 4.10	2.083 ± 0.294
50_AgNPs@PET/SCGs	50	41.54 ± 5.32	5.417 ± 0.779
100_AgNPs@PET/SCGs	100	54.25 ± 8.22	7.292 ± 0.294

3. Results and discussion

3.1. *Characterization of AgNPs@PET/SCGs composites*

In this study, the prepared AgNPs@PET/SCGs composites were subsequently immersed into different $AgNO_3$ solutions (1, 10, 50, and 100 mM) for 6 h to investigate if the AgNPs can be generated on the composites and discuss the effect of concentrations of $AgNO_3$ on the amount of AgNPs. First, the TFA was used as solvent to dissolve PET. When the SCGs and salts were added in the polymer solution, the solution became a "mud". After casting and removing solvent, the PET can trap SCGs in the polymer matrix to form PET/SCGs films (as see in Fig. 2a). Because the SCGs contain large amounts of phenolic compounds which play a role in reducing agents (Chien et al., 2019), the SCGs in the PET/SCGs composites can reduce silver ion to silver nanoparticles to obtain the AgNP@PET/SCGs composites (Fig. 2b–e). They were then characterized by FESEM and XRD. The FESEM result of is depicted in Fig. 3, while the size of silver nanoparticles on AgNPs@PET/SCGs is tabulated in Table 1. It is shown that PET/SCGs composites had a rough surface with porous structures, as observed by FESEM (Fig. 3a). The FESEM images of AgNPs@PET/SCGs clearly show that the formation of some of the bright spots with an average particle size of 34.6 nm on the surfaces of the PET/SCGs composites prepared by using 1 mM $AgNO_3$ (Fig. 3b).The coverage of the bright spots on the surfaces of the PET/SCGs composites is bigger and denser when increasing the concentration of the Ag^+ ions

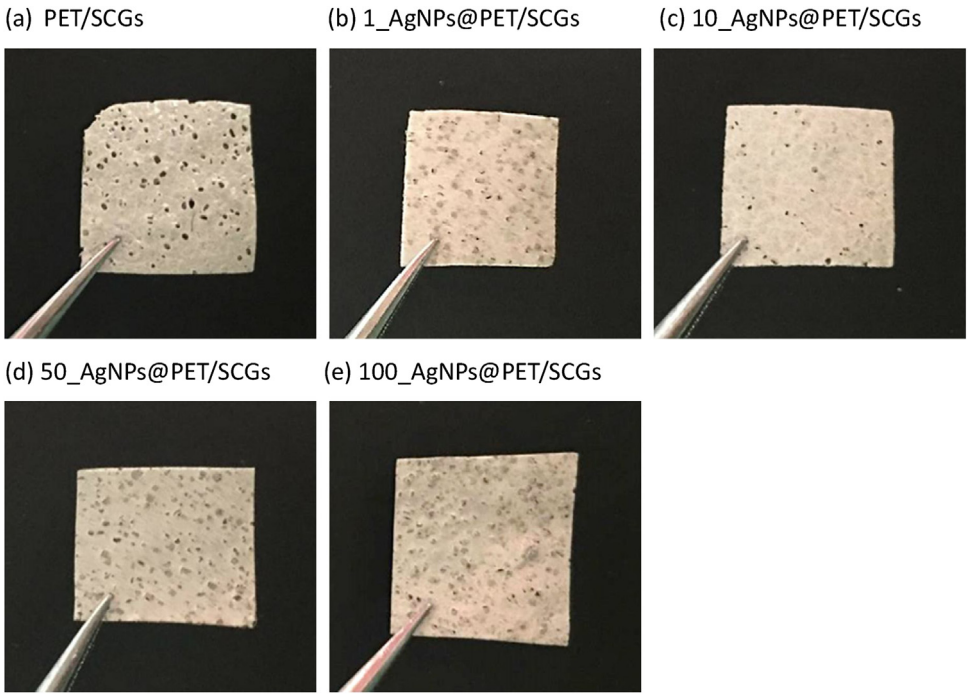

Fig. 2 – The photographs of AgNPs@PET/SCGs composites.
(a) PET/SCGs (b) 1_AgNPs@PET/SCGs (c) 10_AgNPs@PET/SCGs (d) 50_AgNPs@PET/SCGs (e) 100_AgNPs@PET/SCGs.

because more Ag^+ ions were reacted and enhanced the yield of AgNPs (Dubey et al., 2010) (Fig. 3c). A small increase in the average particle size of AgNPs to 38.8 nm at 10_AgNPs@PET/SCGs is observed. The small bright spots began to form clusters when the reaction concentration of $AgNO_3$ increased to 50 mM (50_AgNPs@PET/SCGs, Fig. 3d). A great number of clusters is observed on the surfaces of the PET/SCGs composites when using 100 mM of $AgNO_3$ (Fig. 3e). The average particle size of AgNPs on 50_AgNPs@PET/SCGs and 100_AgNPs@PET/SCGs are 41.5 and 54.2 nm, respectively.

The small bright spots and clusters on AgNPs@PET/SCGs shown in Fig. 3 could represent the existence of crystalline silver nanoparticles. Therefore, the samples were analyzed by using XRD. The XRD patterns of AgNPs@PET/SCGs show several intense peaks at 2θ = 22°, 28°, 32°, 38°, 44°, 64°, and 75°, which were attributed to amorphous PET, crystalline AgCl (111) and (200), Ag (111), (200), (220) and (311), respectively (Fig. 4). The amorphous peak at 2θ = 22° in Fig. 4 might probably correspond to the cellulose of SCGs (Ballestero et al., 2015). We infer that the AgCl peaks (θ = 28 and 32°) might be resulted from the contribution of the residual Cl^- and Ag^+ ions in the initial PET/SCGs solution in TFA which led to the heterogeneous nucleation and the growth of AgCl on the PET/SCGs composites (Zhang et al., 2017). Interestingly, the AgCl peak at 2θ = 28° and 32° gradually decreased when the $AgNO_3$ concentration increased to 50 mM and 100 mM. The decrease of the peak intensity may be due to the increase of $AgNO_3$ concentration which interfered with the crystalline state of AgCl. However, the $AgNO_3$ concentration did not effect on the peak intensities of Ag, indicating that the crystallinity of Ag did not influence by $AgNO_3$ concentration. Despite the detected AgCl characteristic peaks, XRD patterns present that there is still face-centered-cubic (FCC) crystalline structure of silver-based peak in comparison with the values reported by the Joint Committee on Powder Diffraction Standards (JCPDS) file No. 84-0713. Therefore, the XRD results confirm the formation of AgNPs on the PET/SCGs composites.

The effect of the concentration of $AgNO_3$ on the loaded amount of AgNPs is evaluated by using ICP-OES, and the result is reported in Table 1. There is no silver detected in PET/SCGs, while the loaded AgNPs contents in AgNPs@PET/SCGs resulted from preparation with 1, 10, 50 and 100 mM $AgNO_3$ were 0.938, 2.083, 5.417 and 7.292 $\mu g/cm^2$, respectively. The AgNPs content against the concentration of $AgNO_3$ is shown in Fig. 5, where a linear relationship between the AgNPs content and the concentration of $AgNO_3$ was observed when the concentration of $AgNO_3$ <50 mM. However, the loading amount became gradually saturated after the $AgNO_3$ concentration is >50 mM.

The $AgNO_3$ concentration usually exerts a significant effect on the nanoparticle size (Dubey et al., 2010; Dhand et al., 2016). Here, a constant area of PET/SCGs was immersed into $AgNO_3$ aqueous solution at different concentration (1, 10, 50, and 100 mM). The average particle size increases slightly with increasing in the molarity due to the availability of more Ag^+ which leads to an increase in the size of silver nanoparticles (Dubey et al., 2010). Interestingly, to some extent, higher concentration of $AgNO_3$ resulted in more aggregated AgNPs. Several previous studies indicated that the concentration of the plant extracts exert a significant effect on the distribution of nanoparticles (Gangula et al., 2011). Most of them used varied the quantity of the plant extracts and kept the $AgNO_3$ concentration constant (Gangula et al., 2011). It is found that the higher concentration of plant extracts had fewer aggregated nanoparticles because of the more amount of functional ligands from the plant extracts that may bind to the surfaces of the nanoparticles and thus provide better stabilization to the nanoparticles (Gangula et al., 2011). Compared to previous studies of the utilization of plant extracts for preparing nanoparticles, in this study the SCGs were embedded in the PET matrix. Because the functional ligands of SCGs are also embedded inside the polymer matrix, there is only a small amount of coffee extract probably leaked into solvent and bond to the surfaces of the AgNPs. Therefore, the aggregated AgNPs were observed on some AgNPs@PET/SCGs composites.

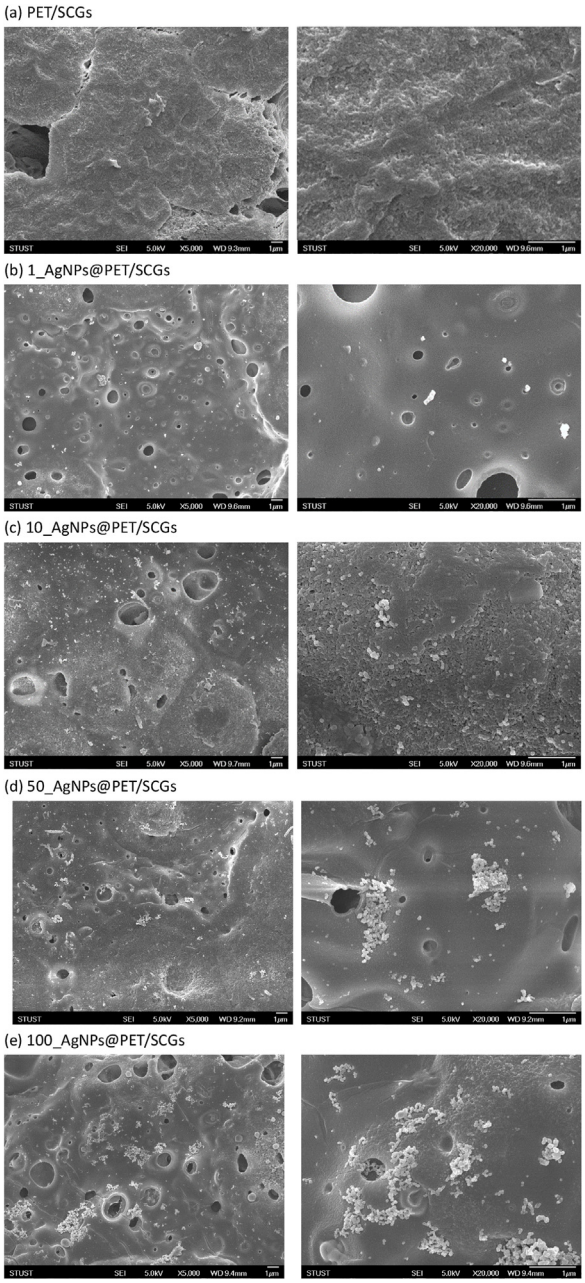

Fig. 3 – FESEM images of (a) PET/SCGs, and AgNPs@PET/SCGs prepared in $AgNO_3$ solution with concentration of (b) 1, (c) 10, (d) 50, and (e) 100 mM.

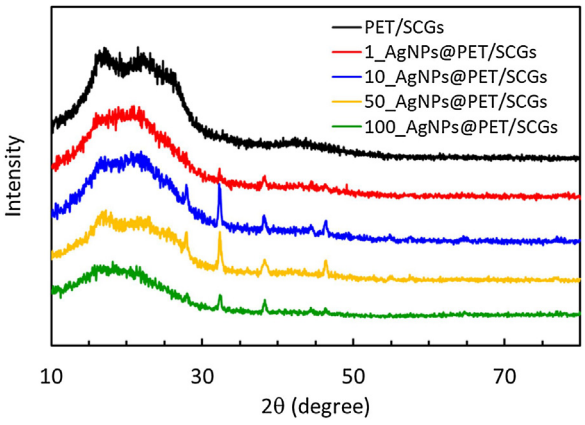

Fig. 4 – XRD patterns of PET/SCGs and AgNPs@PET/SCGs prepared 1 mM, 10 mM, 50 mM, and 100 mM of $AgNO_3$ solution.

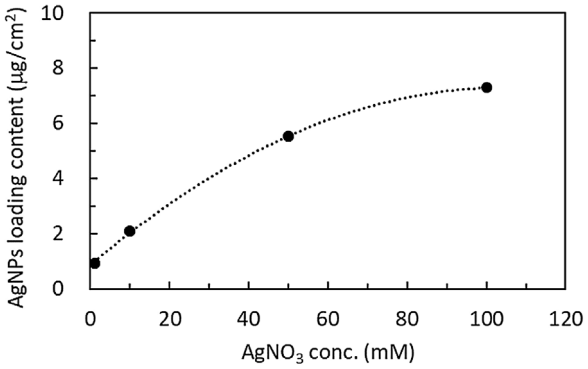

Fig. 5 – Plot the value of AgNPs content against the concentration of $AgNO_3$.

3.2. *Catalytic activity*

Metal nanoparticles have been shown as atom-efficient materials with high density of active sites available for catalysis (Cao et al., 2017; de Souza et al., 2017; Quadrado et al., 2019). Among various metal nanoparticles, AgNPs have been popularly used as catalysis for the reduction high-toxic 4-NP to low-toxic 4-AP (Baruah et al., 2013; Cao et al., 2017; Belachew et al., 2019). In order to demonstrate that the AgNPs synthesized by using coffee-derived composites display the characteristic interfacial chemistry of metallic nanoparticles, and also to support sustainable environment, the reaction of 4-NP reduced by $NaBH_4$ into 4-AP is chosen as a model reaction to analyst the catalytic performance of the biogenic AgNPs@PET/SCGs composites. The yellowish 4-NP serves as a raw material for fungicide for leather, dyes or pigment industries, and especially in pharmaceuticals for the production of acetaminophen (better known as paracetamol, a common analgesic and antipyretic drug) (Bhatti et al., 2002; Vaidya et al., 2003). However, 4-NP is toxic not just for plants and animals, but also to human health (Bhatti et al., 2002). Therefore, its reduction is imperative for better environment and health.

As AgNPs@PET/SCGs composites immersed in 4-NP solution, it is observed that the yellowish solution gradually decolorized to be transparent as the catalytic composites are immersed in the reaction system, suggesting successful reduction of 4-NP. The change in color was further detected by UV–vis spectroscopy in the range of 250–550 nm wavelength at various times, and reported in Fig. 6. The spectra of the 4-NP solution mixed with $NaBH_4$ reducing agent and the non-functionalized PET/SCGs (without AgNPs) show no change over various reaction times. Thus, it is confirmed that $NaBH_4$ by itself was unable to reduce the 4-NP to 4-AP (Fig. 6a). As predicted, the AgNPs@PET/SCGs composites show the decrease of absorbance of 400 nm peak, verifying the successful reduction of 4-NP. Moreover, a new peak emerged at 295 nm with increased reaction time (Fig. 6b–e). It is the fingerprint of 4-AP (Dowle et al., 1990; Baruah et al., 2013; Zhang et al., 2017; Eisa et al., 2018), and therefore confirmed the formation of 4-AP from the reduction of 4-NP, in the presence of $NaBH_4$. This behavior is expected because the AgNPs on the PET/SCGs composites adsorb hydrogen from the $NaBH_4$ and efficiently release it through the reduction reaction. Hence, AgNPs act as a hydrogen carrier between the $NaBH_4$ and the 4-NP (Hervés et al., 2012; Nemanashi and Meijboom, 2013; Gu et al., 2014).

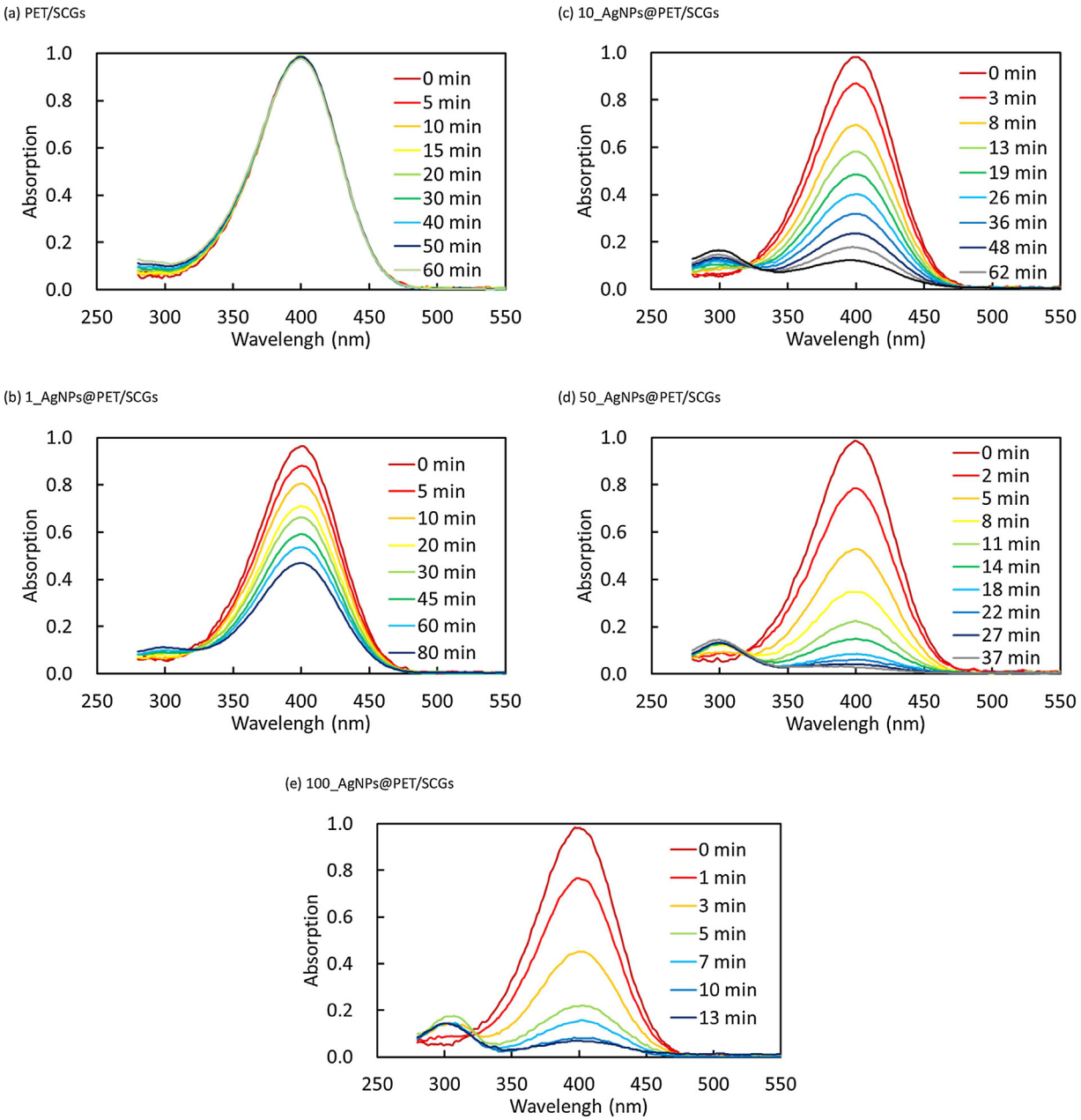

Fig. 6 – UV–vis spectra of reaction systems were recorded by PET/SCGs (a) and AgNPs@PET/SCGs prepared in 1 mM (b), 10 mM (c), 50 mM (d) and 100 mM (e) of $AgNO_3$ solution.

In order to quantitatively describe the catalytic activity of different amount of AgNPs on PET/SCGs composites, the conversion of 4-NP to 4-AP is calculated by Eq. (1):

$$Conversion = \left(1 - \frac{A_t}{A_0}\right) \times 100\% \quad (1)$$

where A_t stands for the absorbance at 400 nm, which is proportional to the concentration of produced 4-NP; A_0 is the initial absorbance at 400 nm after addition of $NaBH_4$. The plots of conversion versus time for different AgNPs@PET/SCGs composites are given in Fig. 7. Without the AgNPs, the conversion was very low and kept unaltered after 60 min for the sample treated by PET/SCGs (Fig. 7a). For various AgNPs@PET/SCGs, the conversion was significantly increased when the reduction reaction developed. At 10 min reaction, the conversion for 1_AgNPs@PET/SCGs, 10_AgNPs@PET/SCGs, 50_AgNPs@PET/SCGs, and 100_AgNPs@PET/SCGs was 16.4%, 33.7%, 73.1%, and 91.9%, respectively, indicating successful catalytic reduction of 4-NP. Furthermore, it is observed that 100_AgNPs@PET/SCGs catalyzed the reaction almost completely within 10 min. In contrast, the catalytic reduction of 50_AgNPs@PET/SCGs is almost completed within 18 min. After 80 min of reaction time, the conversion for 1_AgNPs and 10_AgNPs only approached to 51.3%and 87.7%, respectively. These results suggested that 100_AgNPs@PET/SCGs has the best catalytic activity, followed by 50_AgNPs@PET/SCGs, 10_AgNPs@PET/SCGs and 1_AgNPs@PET/SCGs.

Since the concentration of $NaBH_4$ greatly exceeds that of 4-NP, this reduction reaction can be assumed to be a pseudo-first-order reaction kinetics equation (Baruah et al., 2013; Zhu et al., 2013), which can be described in Eq. (2) as follows:

$$\ln\left(\frac{C_t}{C_0}\right) = -kt \quad (2)$$

where C_0 is the initial concentration, C_t is the concentration at time t, and k is the first-order rate constant of the chemi-

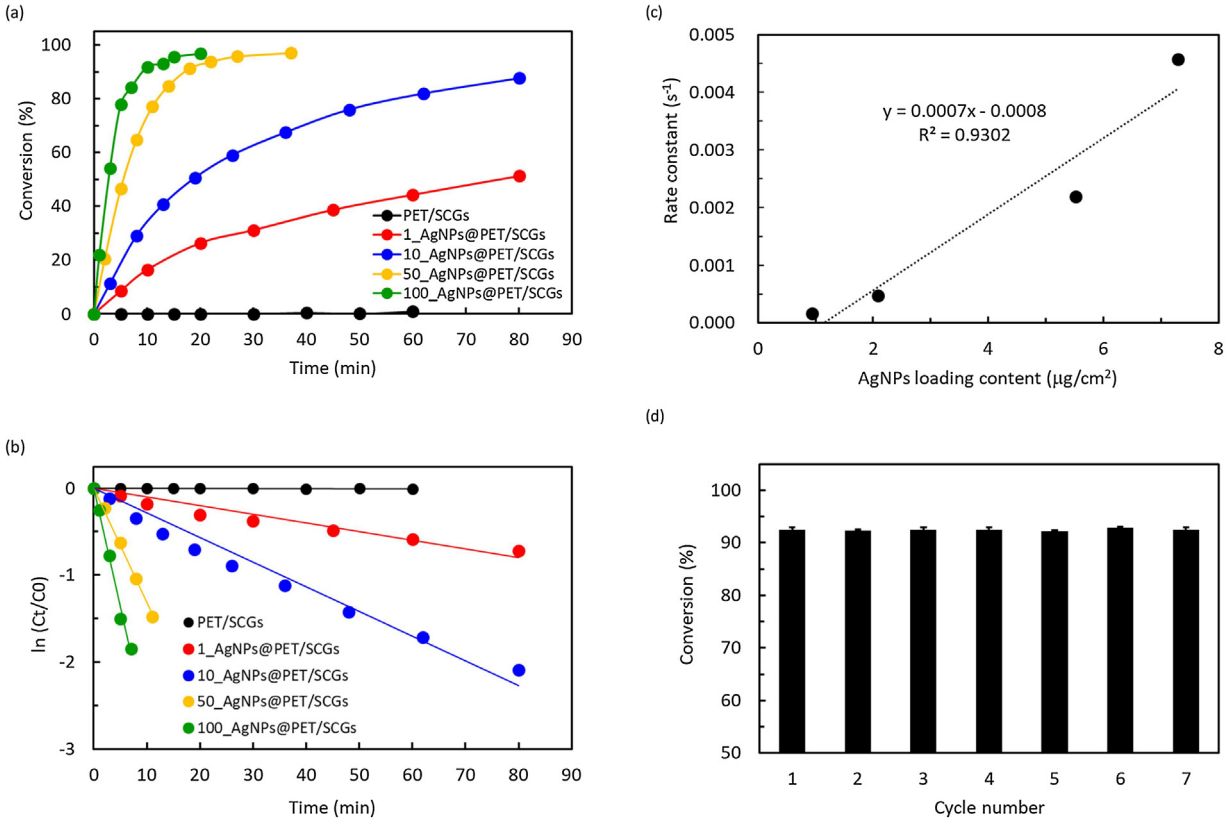

Fig. 7 – Plots of conversion (a) and ln(Ct/C0) (b) against the reaction time for pseudo-first-order reduction kinetics of 4-nitrophenol in the presence of excess $NaBH_4$. (c) A linear relationship between the rate constant *k* and the AgNPs loading content. (d) The recyclability of the 100_AgNPs@PET/SCGs as the catalyst for the reduction of 4-nitrophenol with $NaBH_4$.

Table 2 – Rate constant of AgNPs@PET/SCGs in degradation of 4-NP.

Samples	Rate constant (s^{-1})
PET/SCGs	1.167×10^{-6}
1_AgNPs@PET/SCGs	1.667×10^{-4}
10_AgNPs@PET/SCGs	4.733×10^{-4}
50_AgNPs@PET/SCGs	2.195×10^{-3}
100_AgNPs@PET/SCGs	4.572×10^{-3}

cal reduction (s^{-1}). The linear relationship between $\ln(C_t/C_0)$ and reaction time shown in Fig. 7b is very well in agreement with the first-order reaction kinetics. From this kinetic curve, the rate constant *k* was obtained and summarized in Table 2. It could be observed that the largest *k* is exhibited by 100_AgNPs@PET/SCGs. Moreover, in order to understand the effect of AgNPs loading towards the reaction rate, the value of rate constants is plotted against the concentration of AgNPs (Fig. 7c). It suggests a linear relationship between the rate constant *k* and the AgNPs loading, where the reaction constant *k* is increased with larger loading AgNPs (hence the increase of the amount of the active side of AgNPs), with best performance is provided by 100_AgNPs@PET/SCGs. Furthermore, the best 100_AgNPs@PET/SCGs was further examined. Its durability is retained almost more than 90% conversion after over seven successive catalytic cycles (Fig. 7d). The findings in this study demonstrated that the firstly reported biogenic AgNPs@PET/SCGs composites produced without any extra capping and reducing agent have promising catalytic performance, convenience in re-collection, and also durability for the reduction of 4-NP.

3.3. *Conclusion*

In this study, we report an environmentally benign, inexpensive and facile method of preparing AgNPs@PET/SCGs catalysts without any additional dispersing, capping and reducing agent at room temperature. The method results in active and robust catalysts for 4-NP reduction towards safe and sustainable ecology. The uniform AgNPs with a narrow size distribution ranging from 35 to 54 nm was achieved on the surface of PET/SCGs via a green synthetic in-situ reduction approach. Results from SEM and ICP analysis demonstrated that the amount, size, and distribution of AgNPs could be easily tuned simply by adjusting the $AgNO_3$ concentration. The AgNPs@PET/SCGs catalyst made from wastes of beverage industries show excellent catalytic performances towards the reduction of 4-NP in the presence of $NaBH_4$, with excellent durability of maintaining >90% conversion for at least seven cycles. Taking into consideration that the coffee residues and PET bottles of the current study have virtually zero cost, the AgNPs@PET/SCGs from those wastes are a great potential in water treatment and other prospective applications.

Acknowledgements

The authors would like to acknowledge the financial support from the National Kaohsiung University of Science and Technology (NKUST) and the Ministry of Science and Technology, Taiwan under Grant MOST 107-2218-E-992-001-MY2.

References

Balakrishnan, M., Batra, V.S., Hargreaves, J.S.J., Pulford, I.D., 2011. Waste materials — catalytic opportunities: an overview of the application of large scale waste materials as resources for catalytic applications. Green Chem. 13, 16–24.

Ballestero, L.F., Cerqueira, M.A., Teixeira, J.A., Mussatto, S.I., 2015. Characterization of polysaccharides extracted from spent coffee grounds by alkali pretreatment. Carbohydr. Polym. 127, 347–354.

Baruah, B., Gabriel, G.J., Akbashev, M.J., Booher, M.E., 2013. Facile synthesis of silver nanoparticles stabilized by cationic polynorbornenes and their catalytic activity in 4-nitrophenol reduction. Langmuir 29, 4225–4234.

Belachew, N., Meshesha, D.S., Basavaiah, K., 2019. Green syntheses of silver nanoparticle decorated reduced graphene oxide using L-methionine as a reducing and stabilizing agent for enhanced catalytic hydrogenation of 4-nitrophenol and antibacterial activity. RSC Adv. 9, 39264–39271.

Bennett, J.A., Wilson, K., Lee, A.F., 2016. Catalytic applications of waste derived materials. J. Mater. Chem. A 4, 3617–3637.

Bhatti, Z.I., Toda, H., Furukawa, K., 2002. *p*-Nitrophenol degradation by activated sludge attached on nonwovens. Water Res. 36, 1135–1142.

Campos-Vega, R., Loarca-Piña, G., Vergara-Castañedac, H., Oomah, B.D., 2015. Spent coffee grounds: a review on current research and future prospects. Trends Food Sci. Technol. 45, 24–36.

Cao, H.L., Huang, H.B., Chen, Z., Karadeniz, B., Lü, J., Cao, R., 2017. Ultrafine silver nanoparticles aupported on a conjugated microporous polymer as high-performance nanocatalysts for nitrophenol reduction. ACS Appl. Mater. Interfaces 9, 5231–5236.

Chavan, A.A., Pinto, J., Liakos, I., Bayer, I.S., Lauciello, S., Athanassiou, A., Fragouli, D., 2016. Spent coffee bioelastomeric composite foams for the removal of Pb^{2+} and Hg^{2+} from water. ACS Sustain. Chem. Eng. 4, 5495–5502.

Chien, H.W., Kuo, C.J., Kao, L.H., Lin, G.Y., Chen, P.Y., 2019. Polysaccharidic spent coffee grounds for silver nanoparticles immobilization as a green and highly efficient biocide. Int. J. Biol. Macromol. 140, 168–176.

de Souza, J.F., da Silva, G.T., Fajardo, A.R., 2017. Chitosan-based film supported copper nanoparticles: a potential and reusable catalyst for the reduction of aromatic nitro compounds. Carbohydr. Polym. 161, 187–196.

Dhand, V., Soumya, L., Bharadwaj, S., Chakra, S., Bhatt, D., Sreedhar, B., 2016. Green synthesis of silver nanoparticles using *Coffea arabica* seed extract and its antibacterial activity. Mater. Sci. Eng. C 58, 36–43.

Dowle, C.J., Malyan, A.P., Matheson, A.M., 1990. Separation of the *ortho*, *meta* and *para* isomers of aminophenol by high-performance liquid chromatography. Analyst 115, 105–107.

Duan, H., Wang, D., Li, Y., 2015. Green chemistry for nanoparticle synthesis. Chem. Soc. Rev. 44, 5778–5792.

Dubey, S.P., Lahtinen, M., Sillanpää, M., 2010. Green synthesis and characterizations of silver and gold nanoparticles using leaf extract of *Rosa rugosa*. Colloids Surf. A 364, 34–41.

Eisa, W.H., Abdelgawad, A.M., Rojas, O.J., 2018. Solid-state synthesis of metal nanoparticles supported on cellulose nanocrystals and their catalytic activity. ACS Sustain. Chem. Eng. 6, 3974–3983.

Gangula, A., Podila, R., Karanam, R.M.L., Janardhana, C., Rao, A.M., 2011. Catalytic reduction of 4-nitrophenol using biogenic gold and silver nanoparticles derived from *Breynia rhamnoides*. Langmuir 27, 15268–15274.

Gu, S., Wunder, S., Lu, Y., Ballauff, M., Fenger, R., Rademann, K., Jaquet, B., Zaccone, A., 2014. Kinetic analysis of the catalytic reduction of 4-nitrophenol by metallic nanoparticles. J. Phys. Chem. C 118, 18618–18625.

Hao, L., Wang, P., Valiyaveettil, S., 2017. Successive extraction of As(V), Cu(II) and P(V) ions from water using spent coffee powder as renewable bioadsorbents. Sci. Rep. 7, 42881.

Hervés, P., Pérez-Lorenzo, M., Liz-Marzán, L., Dzubiella, J., Lu, Y., Ballauff, M., 2012. Catalysis by metallic nanoparticles in aqueous solution: model reactions. Chem. Soc. Rev. 41, 5577–5587.

Iravani, S., 2011. Green synthesis of metal nanoparticles using plants. Green Chem. 13, 2638–2650.

Kemp, K.C., Baek, S.B., Lee, W.G., Meyyappan, M., Kim, K.S., 2015. Activated carbon derived from waste coffee grounds for stable methane storage. Nanotechnology 26, 385602.

Klose, F., Scholz, P., Kreisel, G., Ondruschka, B., Kneise, R., Knopf, U., 2000. Catalysts from waste materials. Appl. Catal. B: Environ. 28, 209–221.

Kovalcik, A., Obruca, S., Marova, I., 2018. Valorization of spent coffee grounds: a review. Food Bioprod. Process 110, 104–119.

Kyzas, G.Z., 2012. Commercial coffee wastes as materials for adsorption of heavy metals from aqueous solutions. Materials 5, 1826–1840.

Lessa, E.F., Nunes, M.L., Fajardo, A.R., 2018. Chitosan/waste coffee-grounds composite: an efficient and eco-friendly adsorbent for removal of pharmaceutical contaminants from water. Carbohydr. Polym. 189, 257–266.

Metz, K.M., Sanders, S.E., Pender, J.P., Dix, M.R., Hinds, D.T., Quinn, S.J., Ward, A.D., Duffy, P., Cullen, R.J., Colavita, P.E., 2015. Green synthesis of metal nanoparticles via natural extracts: the biogenic nanoparticle corona and its effects on reactivity. ACS Sustain. Chem. Eng. 3, 1610–1617.

Mittal, A.K., Chisti, Y., Banerjee, U.C., 2013. Synthesis of metallic nanoparticles using plant extracts. Biotechnol. Adv. 31, 346–356.

Mussatto, S.I., Ballesteros, L.F., Martin, S., Teixeira, J.A., 2011. Extraction of antioxidant phenolic compounds from spent coffee grounds. Sep. Purif. Technol. 83, 173–179.

Nadagouda, M.N., Varma, R.S., 2008. Green synthesis of silver and palladium nanoparticles at room temperature using coffee and tea extract. Green Chem. 10, 859–862.

Nemanashi, M., Meijboom, R., 2013. Synthesis and characterization of Cu, Ag and Au dendrimer-encapsulated nanoparticles and their application in the reduction of 4-nitrophenol to 4-aminophenol. J. Colloid Interface Sci. 389, 260–267.

Quadrado, R.F.N., Gohlke, G., Oliboni, R., Smaniotto, A., Fajardo, A.R., 2019. Hybrid hydrogels containing one-step biosynthesized silver nanoparticles: preparation, characterization and catalytic application. J. Ind. Eng. Chem. 79, 326–337.

Saratale, R.G., Saratale, G.D., Cho, S.K., Ghodake, G.S., Kadam, A.A., Kumar, S., Mulla, S.I., Kim, D.S., Jeon, B.H., Chang, J.S., Shin, H.S., 2019. Phyto-fabrication of silver nanoparticles by *Acacia nilotica* leaves: investigating their antineoplastic, free radical scavenging potential and application in H_2O_2 sensing. J. Taiwan Inst. Chem. Eng. 99, 239–249.

Sharma, V.K., Yngard, R.A., Lin, Y., 2009. Silver nanoparticles: green synthesis and their antimicrobial activities. Adv. Colloid Interface Sci. 145, 83–96.

Thanh, N.T.K., Maclean, N., Mahiddine, S., 2014. Mechanisms of nucleation and growth of nanoparticles in solution. Chem. Rev. 114, 7610–7630.

Vaidya, M.J., Kulkarni, S.M., Chaudhari, R.V., 2003. Synthesis of *p*-aminophenol by catalytic hydrogenation of *p*-nitrophenol. Org. Process Res. Dev. 7, 202–208.

Veisi, H., Farokhia, M., Hamelian, M., Hemmati, S., 2018. Green synthesis of Au nanoparticles using an aqueous extract of *Stachys lavandulifolia* and their catalytic performance for alkyne/aldehyde/amine A3 coupling reactions. RSC Adv. 8, 38186–38195.

Xiong, X., Yu, I.K.M., Tsang, D.C.W., Bolan, N.S., Ok, Y.S., Igalavithana, A.D., Kirkham, M.B., Kim, K.H., Vikrant, K., 2019. Value-added chemicals from food supply chain wastes: state-of-the-art review and future prospects. Chem. Eng. J. 375, 121983.

Yeung, P.T., Chung, P.Y., Tsang, H.C., Tang, J.C.O., Cheng, G.Y.M., Gambari, R., Chui, C.H., Lam, K.H., 2014. Preparation and characterization of bio-safe activated charcoal derived from coffee waste residue and its application for removal of lead and copper ions. RSC Adv. 4, 38839–38847.

Zhang, Y., Filipczak, P., He, G., Nowaczyk, G., Witczak, L., Raj, W., Kozanecki, M., Matyjaszewski, K., Pietrasik, J., 2017. Synthesis and characterization of Ag NPs templated via polymerization induced self-assembly. Polymer 129, 144–150.

Zhu, M., Wang, C., Meng, D., Diao, G., 2013. In situ synthesis of silver nanostructures on magnetic Fe3O4@C core–shell nanocomposites and their application in catalytic reduction reactions. J. Mater. Chem. A 1, 2118–2125.

Zuorro, A., Lavecchia, R., 2012. Spent coffee grounds as a valuable source of phenolic compounds and bioenergy. J. Clean. Prod. 34, 49–56.